Насыщенные внутренние волны в атмосфере Марса по данным анализа радиозатменных измерений

Губенко В.Н., Кириллович И.А., Андреев В.Е., Губенко Т.В., Павельев А.А., Губенко Д.В.

ФИРЭ им. В.А. Котельникова РАН, пл. акад. Б.А. Введенского д.1, 141190 Фрязино, Московская обл., Россия

e-mail: vngubenko@gmail.com

Четырнадцатая Всероссийская открытая конференция "Современные проблемы дистанционного зондирования Земли из космоса“

14 - 18 ноября 2016 года, Москва

Введение

Волновые процессы оказывают значительное влияние на циркуляцию, химический состав и тепловой режим атмосферы Марса. Важная роль внутренних гравитационных волн (ВГВ), в первую очередь, связана с обеспечением ими эффективного механизма переноса энергии и горизонтального импульса из нижних уровней атмосферы на верхние. Источником генерации ВГВ в атмосфере могут являться: тепловые контрасты вблизи поверхности, топография, сдвиговая неустойчивость ветра, конвекция и фронтальные процессы. В атмосфере Земли в отсутствие диссипации энергии, амплитуда волновых возмущений скорости ветра или температуры растет примерно экспоненциально с увеличением высоты и поэтому возмущения с малой амплитудой вблизи поверхности могут производить значительные эффекты на больших высотах, где происходит обрушение волн и передача энергии и горизонтального импульса ВГВ в невозмущенный поток. Поскольку внутренние гравитационные волны являются характерной особенностью устойчиво стратифицированной атмосферы **[*Gubenko et al*., 2008a, 2011, 2012]**, то аналогичные эффекты можно ожидать в атмосферах Венеры и Марса **[*Gubenko et al*., 2008b, 2015].** Полагают, что внутренние волны могут играть более важную роль в формировании циркуляции, теплового режима и структуры атмосферы на Марсе, чем на Земле, так как во многих случаях амплитуды ВГВ в атмосфере Марса оказываются существенно больше своих земных аналогов **[*Fritts et al*., 2006].** Нами разработан оригинальный метод идентификации дискретных (узкоспектральных) волновых событий и определения характеристик внутренних гравитационных волн на основе анализа вертикального профиля температуры, плотности или квадрата частоты Брента-Вяйсяля в атмосфере планеты **[*Gubenko et al*., 2008a, 2011, 2012, 2015].** Сформулирован и обоснован пороговый критерий идентификации ВГВ, в случае выполнения которого анализируемые флуктуации могут рассматриваться как волновые проявления. Показано, что данный метод исследования волновых процессов можно применять для анализа вертикальных профилей температуры или плотности, полученных любыми способами как в атмосфере Земли, так и в атмосферах Венеры и Марса.

Цель работы:

Проведение обработки и анализа вертикальных профилей температуры, восстановленных из радиозатменых измерений миссии *MARS GLOBAL SURVEYOR*, для идентификации дискретных волновых событий и реконструкции характеристик внутренних гравитационных волн в атмосфере Марса.

Method for investigations of discrete wave events

$N_b^2 >> \omega^2 > f^2$ ***Approximation for medium- and low-frequency waves***

$$\left| c_h - \bar{u} \right|^2 = \frac{\omega^2}{k_h^2} = \frac{N_b^2}{m^2} \cdot \frac{1}{1 - f^2/\omega^2}$$

Dispersion relation for IGWs

Polarization equation for IGWs

$$\left| u' \right| = \frac{g}{N_b} \cdot \frac{\left| T' \right|}{T_b} \cdot \left(1 - f^2/\omega^2\right)^{-1/2}$$

Relative amplitude threshold for shear instability [*Fritts*, 1989]

$$a = \frac{\left| u'_{sat} \right|}{\left| c_h - \bar{u} \right|} = \frac{2 \cdot \left(1 - f^2/\omega^2\right)^{1/2}}{1 + \left(1 - f^2/\omega^2\right)^{1/2}}$$

Brunt-Vaisala frequency squared

$$N_b^2 = \frac{g}{T_b} \cdot \left(\frac{\partial T_b}{\partial z} + \frac{g}{c_p} \right)$$

Actual wave amplitude (hypothetic) found from experiment

[*Gubenko et al.*, 2008a, 2011, 2012, 2015]

$$a_e = \frac{\left| u' \right|}{\left| c_h - \bar{u} \right|} = \frac{g \left| m \right|}{N_b^2} \cdot \frac{\left| T' \right|}{T_b} = A_{N^2}^{\mathrm{rel}} = 1 - \frac{N_{min}^2}{N_b^2}$$

Coriolis parameter (inertial frequency)

$f = 2\Omega \cdot \sin \varphi$

Criterion for the IGW identification

$$1 > a = a_e > 0$$

Sketch of the IGW parameter reconstruction from an analysis of the vertical temperature profile in a planetary atmosphere

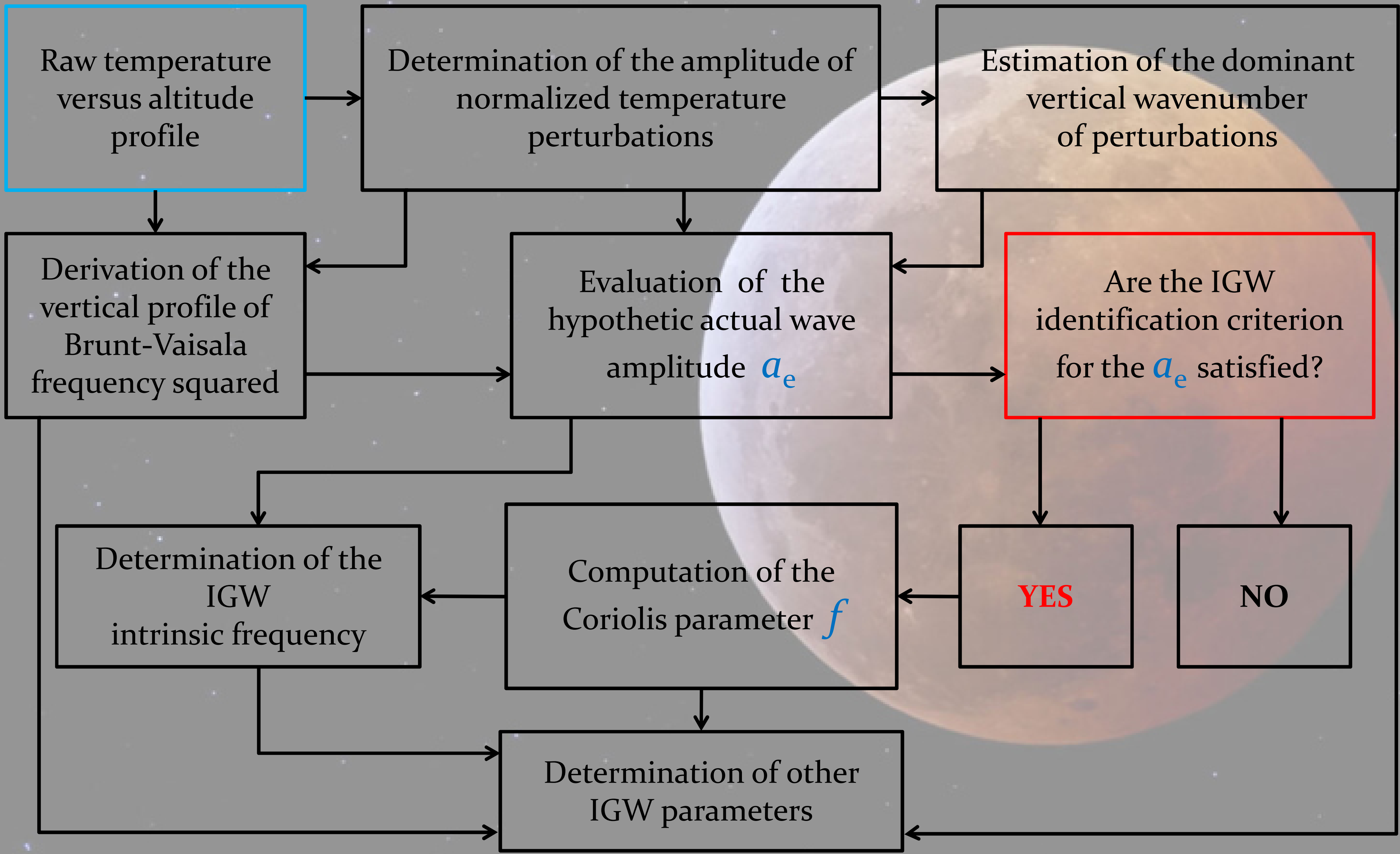

Determined IGW parameters [*Gubenko et al.*, 2008a]

Intrinsic frequency

$$\omega = \frac{f}{2}\cdot\frac{2-a_e}{(1-a_e)^{1/2}}$$

Horizontal wave number

$$|k_h| = \frac{\omega}{|c_h-\bar{u}|} = \frac{|m|}{2}\cdot\frac{f}{N_b}\cdot\frac{a_e}{(1-a_e)^{1/2}} = \frac{\pi\cdot f}{\lambda_z N_b}\cdot\frac{a_e}{(1-a_e)^{1/2}}$$

Intrinsic horizontal phase speed

$$\left|C_{ph}^{in}\right| = |c_h-\bar{u}| = \frac{N_b}{|m|}\cdot\frac{2-a_e}{a_e} = \frac{\lambda_z N_b}{2\pi}\cdot\frac{2-a_e}{a_e}$$

Horizontal wavelength

$$\lambda_h = \frac{2\pi}{|k_h|} = 4\pi\frac{N_b}{f}\cdot\frac{(1-a_e)^{1/2}}{a_e\cdot|m|} = 2\frac{\lambda_z N_b}{f}\cdot\frac{(1-a_e)^{1/2}}{a_e}$$

Intrinsic vertical phase speed

$$\left|C_{pz}^{in}\right| = \frac{\omega}{|m|} = \frac{f}{2|m|}\cdot\frac{2-a_e}{(1-a_e)^{1/2}} = \frac{\lambda_z f}{4\pi}\cdot\frac{2-a_e}{(1-a_e)^{1/2}}$$

Amplitude of vertical perturbations of wind speed

$$|w'| = \frac{|k_h|}{|m|}\cdot|u'| = \frac{f\cdot a_e}{2|m|}\cdot\frac{2-a_e}{(1-a_e)^{1/2}} = \frac{\lambda_z f\cdot a_e}{4\pi}\cdot\frac{2-a_e}{(1-a_e)^{1/2}}$$

Amplitudes of horizontal perturbations of wind speed

$$|u'| = a_e|c_h-\bar{u}| = \frac{N_b}{|m|}\cdot(2-a_e) = \frac{\lambda_z N_b}{2\pi}\cdot(2-a_e)$$

$$|v'| = \frac{f}{\omega}\cdot|u'| = 2\frac{N_b}{|m|}(1-a_e)^{1/2} = \frac{\lambda_z N_b}{\pi}(1-a_e)^{1/2}$$

in the direction of horizontal component of wave vector

in the direction normal to horizontal component of wave vector

Energy IGW parameters [*Gubenko et al.*, 2011]

$$\tan \varphi' = \frac{|m|}{|k_h|} = \frac{\lambda_h}{\lambda_z}$$ *Tan of the angle between wave vector and horizontal plane*

Wave kinetic energy per unit mass $$E_k = \frac{1}{2}\left[\overline{u'^2} + \overline{v'^2} + \overline{w'^2}\right] = E \cdot \frac{1 + (f/\omega)^2 \sin^2 \varphi'}{2}$$

Wave potential energy per unit mass

$$E_p = \frac{1}{2}\frac{g^2}{N_b^2}\overline{\left(\frac{T'}{T_b}\right)^2} = \frac{1}{4}\frac{g^2}{N_b^2}\left|\frac{T'}{T_b}\right|^2 = E \cdot \frac{1 - (f/\omega)^2 \sin^2 \varphi'}{2}$$

$$E = E_k + E_p = \frac{1}{2}|w'|^2\left(1 + \mathrm{tg}^2\varphi'\right) = \frac{1}{2}\left(|w'|^2 + |u'|^2\right)$$ *Total wave energy per unit mass*

Ratio of kinetic to potential energy $$p = \frac{E_k}{E_p} = \frac{\omega^2 + f^2 \sin^2 \varphi'}{\omega^2 - f^2 \sin^2 \varphi'} = 1 + 2\frac{f^2}{N_b^2}\mathrm{tg}^2\varphi'$$

$$\left|C_{gh}^{in}\right| = \left|\frac{\partial \omega}{\partial k_h}\right| = \left|C_{ph}^{in}\right| \cdot \left(1 - \frac{f^2}{\omega^2}\right) = \frac{N_b}{|m|} \cdot \sqrt{1 - \frac{f^2}{\omega^2}}$$ *Intrinsic horizontal group speed*

Intrinsic vertical group speed $$\left|C_{gz}^{in}\right| = \left|\frac{\partial \omega}{\partial m}\right| = \left|C_{pz}^{in}\right| \cdot \left(1 - \frac{f^2}{\omega^2}\right) = \frac{|k_h| N_b}{m^2} \cdot \sqrt{1 - \frac{f^2}{\omega^2}}$$

Fluxes of the wave energy and horizontal momentum [*Gubenko et al.*, 2011]

$$\left|\frac{C_{gz}^{in}}{C_{gh}^{in}}\right| = \left|\frac{C_{pz}^{in}}{C_{ph}^{in}}\right| = \left|\frac{k_h}{m}\right| = \frac{\lambda_z}{\lambda_h} = \frac{\omega}{N_b}\cdot\sqrt{1-\frac{f^2}{\omega^2}}$$

Ratio of vertical to horizontal group (phase) speed

$$\left|F_z\right| = \left|C_{gz}^{in}\right|\cdot E$$

Vertical flux of wave energy

$$\left|F_h\right| = \left|C_{gh}^{in}\right|\cdot E$$

Horizontal flux of wave energy

Total vertical flux of horizontal momentum due to IGW

$$\left|F_{ph}\right| = \sqrt{\left(\overline{u'\cdot w'}\right)^2 + \left(\overline{v'\cdot w'}\right)^2} = \left|\overline{u'\cdot w'}\right| = \frac{\left|u'\right|\cdot\left|w'\right|}{2} = \left|\frac{k_h}{m}\right|\cdot\frac{\left|u'\right|^2}{2}$$

Errors of the actual wave amplitude determination
[*Gubenko et al.*, 2008a, 2012]

$$a_e = \frac{|u'|}{|c-\bar{u}|} = \frac{g|m|}{N_b^2}\cdot\frac{|T'|}{T_b} = \frac{2\pi\cdot g}{\lambda_z N_b^2}\cdot\frac{|T'|}{T_b} = a = \frac{2\left(1-f^2/\omega^2\right)^{1/2}}{1+\left(1-f^2/\omega^2\right)^{1/2}}$$

Actual wave amplitude

Relative uncertainty of the actual wave amplitude determination

$$X = \frac{\delta a_e}{a_e} \approx \left[\left(\frac{\delta|T'|}{|T'|}\right)^2 + \left(\frac{\delta\lambda_z}{\lambda_z}\right)^2 + \left(\frac{\delta N_b^2}{N_b^2}\right)^2\right]^{1/2} \approx \left[\frac{\lambda_z}{L}\left(\frac{\delta T}{|T'|}\right)^2 + \frac{\lambda_z}{L}\left(\frac{\delta h}{\lambda_z}\right)^2 + \left(\frac{\delta N_b^2}{N_b^2}\right)^2\right]^{1/2}$$

$1 > a = a_e > 0$ ***Theoretical limitation for the amplitude threshold*** a

Restrictions for the actual wave amplitude determined from the real experiment

$$1 > a_e + \delta a_e > a_e > a_e - \delta a_e > 0 \quad \Leftrightarrow \quad 1 > (1+X)\, a_e > a_e > (1-X)\, a_e > 0$$

Minimal amplitude of temperature perturbations applicable to identify IGW

$$\min|T'| = \delta T \,/\, [L/\lambda_z - (\delta h/\lambda_z)^2]^{1/2}$$

Wave observations in the Earth's polar atmosphere on 07 Apr 2001

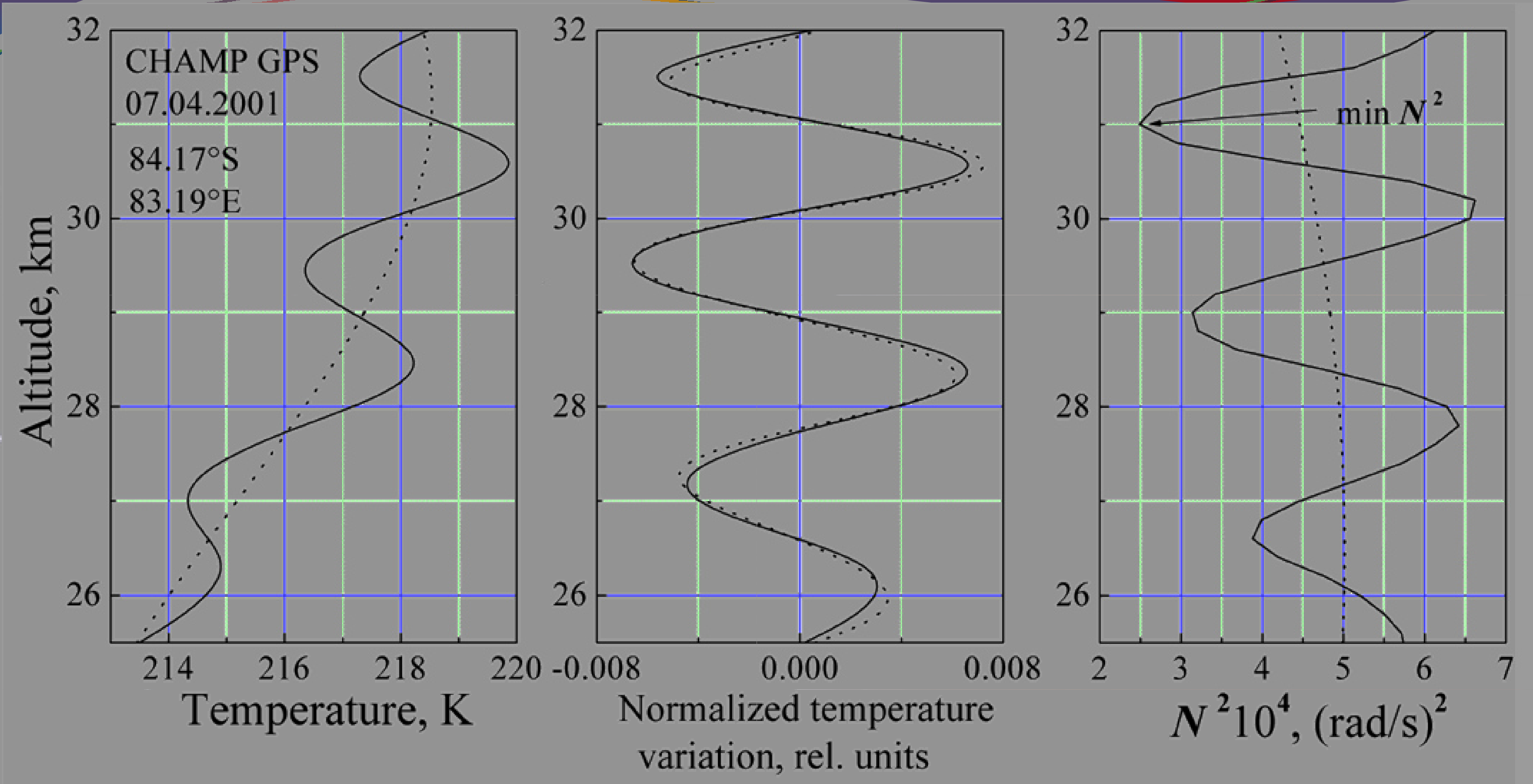

Figure 1. Wave-like perturbations observed 07 April 2001 in the high southern latitudes of the Earth's atmosphere from the *CHAMP* GPS RO vertical temperature profile. In successive panels the vertical profiles of temperature (left), normalized temperature variation (middle), and Brunt-Vaisala frequency squared N^2 (right) are plotted. Solid and dotted lines represent the raw and background data, correspondingly. Background profiles were determined by a least-squares cubic polynomial fit of raw data within the selected altitude interval from 25.5 to 32 km of wave observations.

Wave observations in the Earth's near-polar atmosphere on 15 Jan 2002

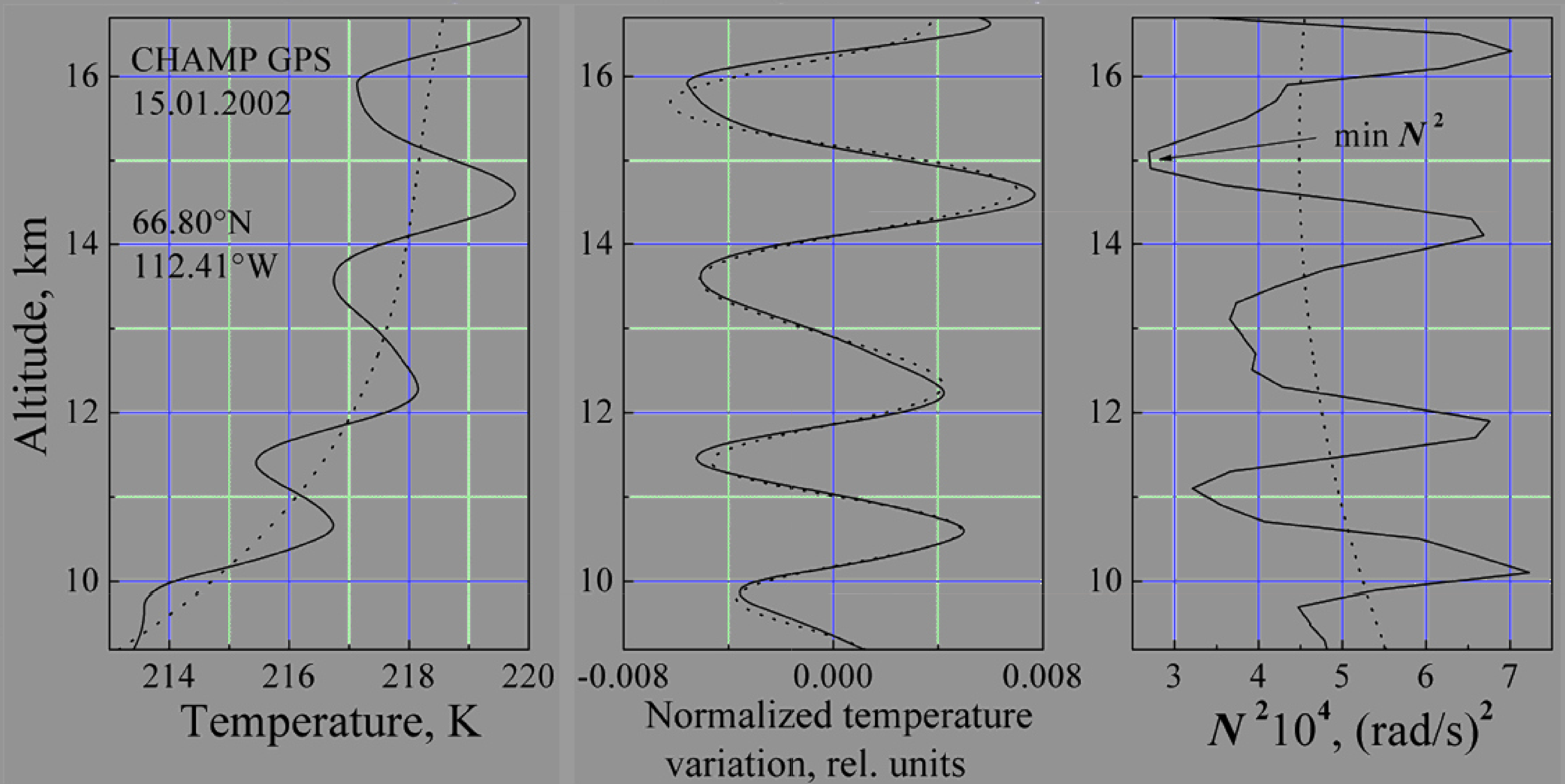

Figure 2. The same as Figure 1, except from radio occultation conducted in the high northern latitudes of the Earth's atmosphere on 15 January 2002.

Experimental data for an internal wave analysis in the Martian atmosphere

The data on the vertical temperature profiles of the *MGS* mission were taken by us from NASA's archive of the planetary data system (http://starbrite.jpl.nasa.gov/pds/… , Planetary Data System) and they were the primary material for processing and analysis in order to identify IGWs and reconstruct wave characteristics in the Martian atmosphere. The vertical resolution of these temperature profiles, which depends on the geometry of the experiment and the wavelength of the sounding signal, is limited by diffraction effects and is ~1 km. Near the planet's surface, where the restored profiles are most accurate, the standard deviation of temperature fluctuations is equal to about 0.4 K, which corresponds to the value of relative data spread of ~0.2% **[*Hinson et al.*, 2001]**. The vertical resolution of the temperature data was significantly different for different profiles, but it was not worse than 1250 m **[*Creasey et al.*, 2006]**. Therefore, to ensure consistency in data processing and to simplify the spectral analysis of investigated fluctuations, the altitude interpolation of temperature values was performed each 1250 m. The high-frequency filtration of temperature fluctuations with a cutoff at 10 km allowed us to exclude structures with the vertical wavelengths more than 10 km, which may not be caused by IGWs but instead by thermal tides, occurring most often in the atmosphere above the mountains, particularly over the Tharsis region **[*Creasey et al.*, 2006]**. At the next step of data processing, the method of an analysis of wave manifestations and IGW parameter determination was applied to the vertical temperature profiles. As can be seen from **[*Gubenko et al.*, 2008a, 2011, 2012]**, in the case of a positive identification of IGWs, we can determine key wave parameters such as the intrinsic frequency, amplitudes of vertical and horizontal disturbances of wind velocity, vertical and horizontal wavelength, intrinsic vertical and horizontal phase velocities, density of kinetic, potential, and total energy, vertical fluxes of wave energy and horizontal momentum, and others. For the further analysis of profiles in order to identify wave events, we have selected vertical profiles where noticeable quasi-periodic temperature variations were observed, and intervals of wave observation were determined for each of the selected profiles **[*Gubenko et al.*, 2015]**.

Example of wave observations in the Martian atmosphere on 28 Jan 1998

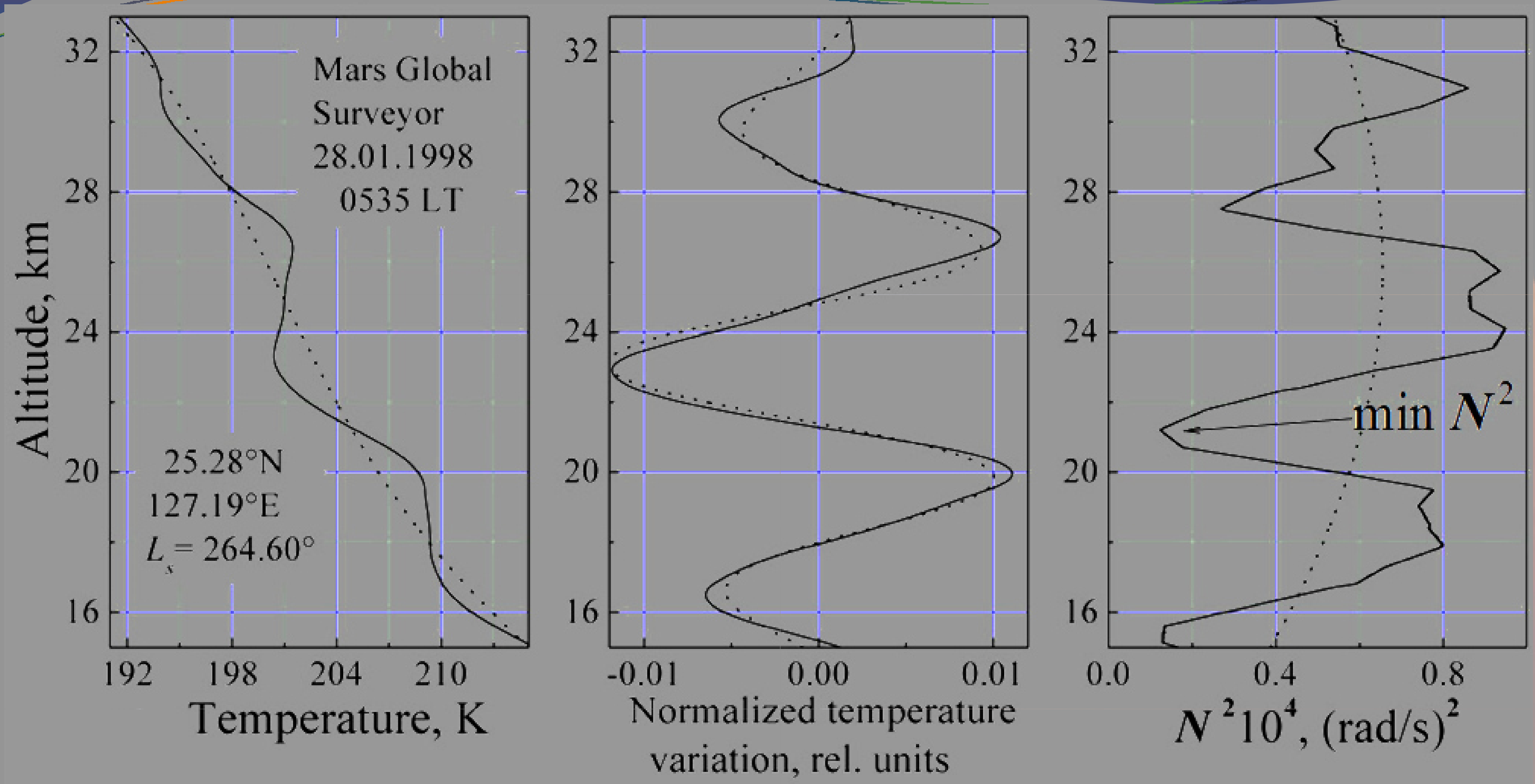

Figure 3. Example of IGW observations in the Martian atmosphere from the vertical temperature profile (data file: 8028X18A .TPS) retrieved from *MGS* radio occultation on 28 January 1998. The season was late fall in the northern hemisphere (celestial longitude L_s=264.60°) and the local true solar time was 05 h 35 m, corresponding to early morning. **Wave parameters:** λ_z=6.8 km; λ_h=1770 km; E=68.6 J/kg; $p=E_k/E_p$=9.2; E_p=6.7 J/kg; f/ω=0.90; $T^{in}=2\pi/\omega$=25.8 hrs; a_e=0.61; $|u'|$=11.7 m/s; $|v'|$=10.5 m/s [*Gubenko et al.*, 2015].

Example of wave observations in the Martian atmosphere on 13 May 1999

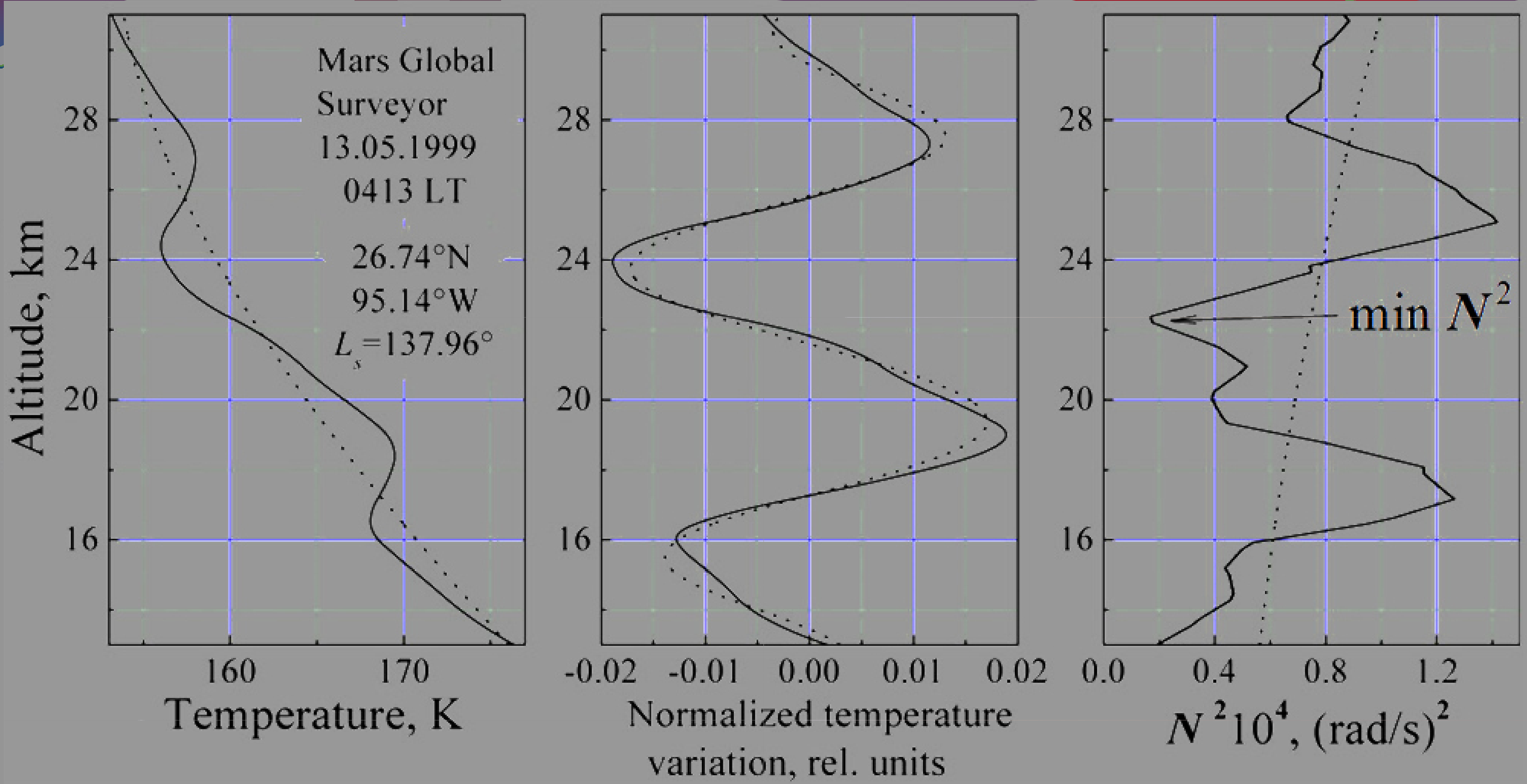

Figure 4. Example of IGW observations in the Martian atmosphere from the vertical temperature profile (data file: 9133B13A .TPS) retrieved from MGS radio occultation on 13 May 1999. The season was summer in the northern hemisphere (celestial longitude L_s=137.96°) and the local true solar time was 04 h 13 m, corresponding to early morning. **Wave parameters:** λ_z=8.2 km; λ_h=2520 km; E=129 J/kg; $p=E_k/E_p$=11.4; E_p=10.4 J/kg; f/ω=0.92; $T^{in}=2\pi/\omega$=25.0 hrs; a_e=0.57; $|u'|$=16.1 m/s; $|v'|$=14.7 m/s [*Gubenko et al.*, 2015].

The case of fully saturated IGW and wave induced turbulence

Figure 5 shows an example of altitude profiles of variations of the temperature and buoyancy frequency square in the range of 8–26.5 km restored from the measurements of the *MGS* mission on 19 May 1999 in the Martian atmosphere. The indicated measurements were performed during the Martian summer (L_s = 141.03°) at 4 h 10 m of local time in the atmospheric region with coordinates 18.11° N and 112.65° W (data file: 9139G18A.TPS) located above the Tharsis mountain volcanic massif. Powerful quasi-periodic variations of T and N^2 with a vertical wavelength of ~6.6 km are identified as manifestations of saturated IGW in the planet's atmosphere. Two independent estimates of the wave amplitude, a_e= 0.95 and $A^{rel}_{N^2}$ = 1, in good agreement with each other, testify that the saturation degree of the wave amplitude is not less than 95%, since for saturated IGW with any intrinsic frequency ω, the relative threshold amplitude does not exceed one. The intrinsic frequency of the internal wave is greater than the inertial frequency approximately by a factor of 2.4 (f/ω = 0.42), and its kinetic energy is greater than potential energy by a factor of 1.4. It is seen from Figure 5 that IGW propagation leads to a strong modulation of the stability of atmospheric stratification. Local values of parameter N^2 reach zero near levels of 9, 15, and 21 km, which assumes here not only dynamic, but also convective instability, and the occurrence of thin layers of intermittent turbulence in the atmosphere. The red circles on Figure 5 indicate possible locations of thin turbulent layers induced by the propagation of saturated internal wave. These thin layers of turbulence having a thickness significantly less than λ_z and a horizontal extent of the order of magnitude of λ_h cannot destroy the structure of the wave field **[*Gubenko et al.*, 2015].**

Manifestation of the fully saturated IGW in the Martian atmosphere

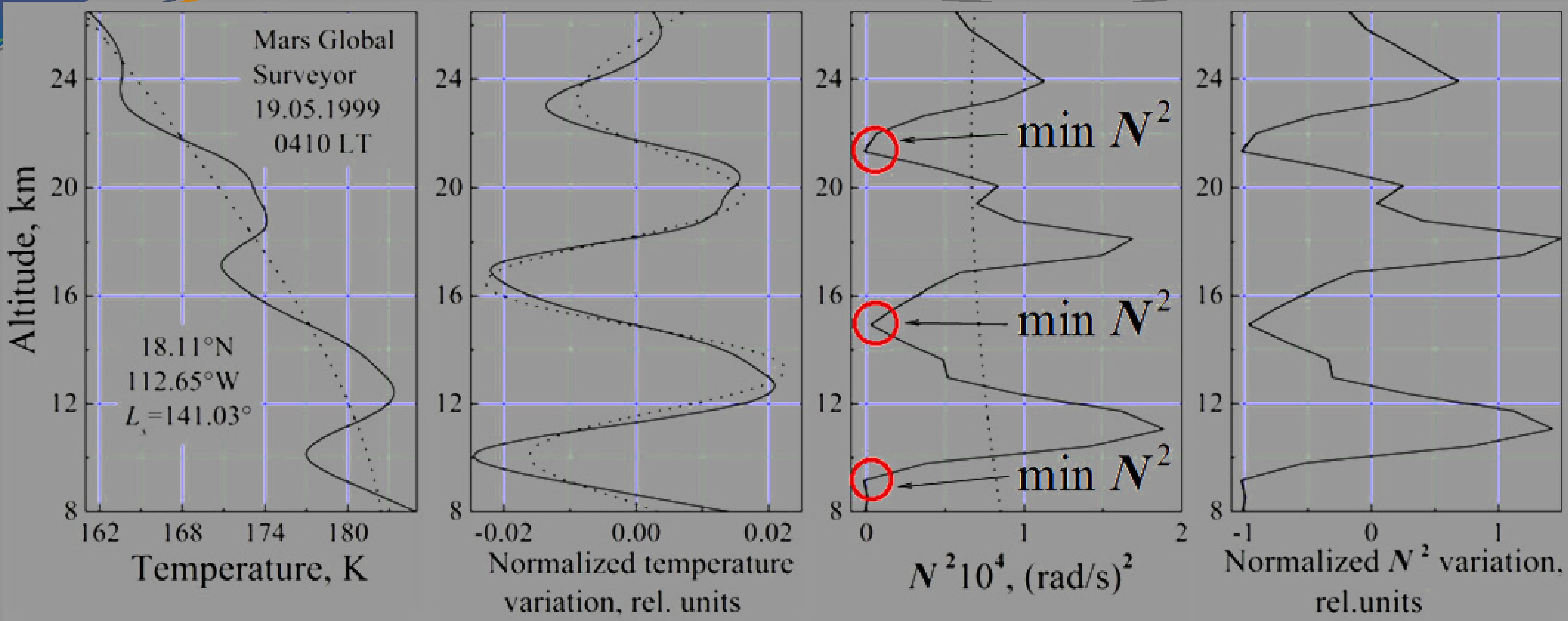

Figure 5. Manifestation of the fully saturated IGW (sat. degree ≥ 0.95) in the Martian atmosphere (Tharsis region) from the vertical temperature profile (data file: 9139G18A.TPS) retrieved from *MGS* RO on 19 May 1999. The season was summer in the northern hemisphere (celestial longitude L_s =141.03°) and the local true solar time was 04:10 h, corresponding to early morning. **Wave parameters:** λ_z=6.6 km; λ_h=580 km; E=42.7 J/kg; $p=E_k/E_p$=1.4; E_p=17.6 J/kg; f/ω=0.42; $T^{in}=2\pi/\omega$=16.6 hrs; a_e=0.95; $|u'|$=9.2 m/s; $|v'|$=3.9 m/s **[*Gubenko et al.*, 2015].**

The case study of so-called "clean" wave observations

Figure 6 shows a rare example of so-called "clean" wave observations, where noise was not discovered in the spectrum of analyzed temperature fluctuations. Coordinates of the probing atmospheric region and information about the time of the measurements are shown in Figure 6. Quasi-periodic variations of T and N^2 with a vertical wavelength of ~4.5 km have been identified as signatures of propagation of inertial IGW in the Martian atmosphere. The intrinsic frequency of the internal wave is close to the inertial frequency ($f/\omega = 0.89$), and its kinetic energy is greater than potential energy by a factor of 8.4. The very good correspondence of the values of the wave parameters reconstructed by two different ways should be noted. We find that the value $A^{rel}_{N^2} = 0.63$ coincides with the estimate of the wave amplitude a_e obtained from an analysis of the temperature data. A comparison shows that the results of reconstruction of the IGW parameters obtained by two different methods are practically identical **[*Gubenko et al.*, 2015].**

Example of “clean” wave observations in the Martian atmosphere

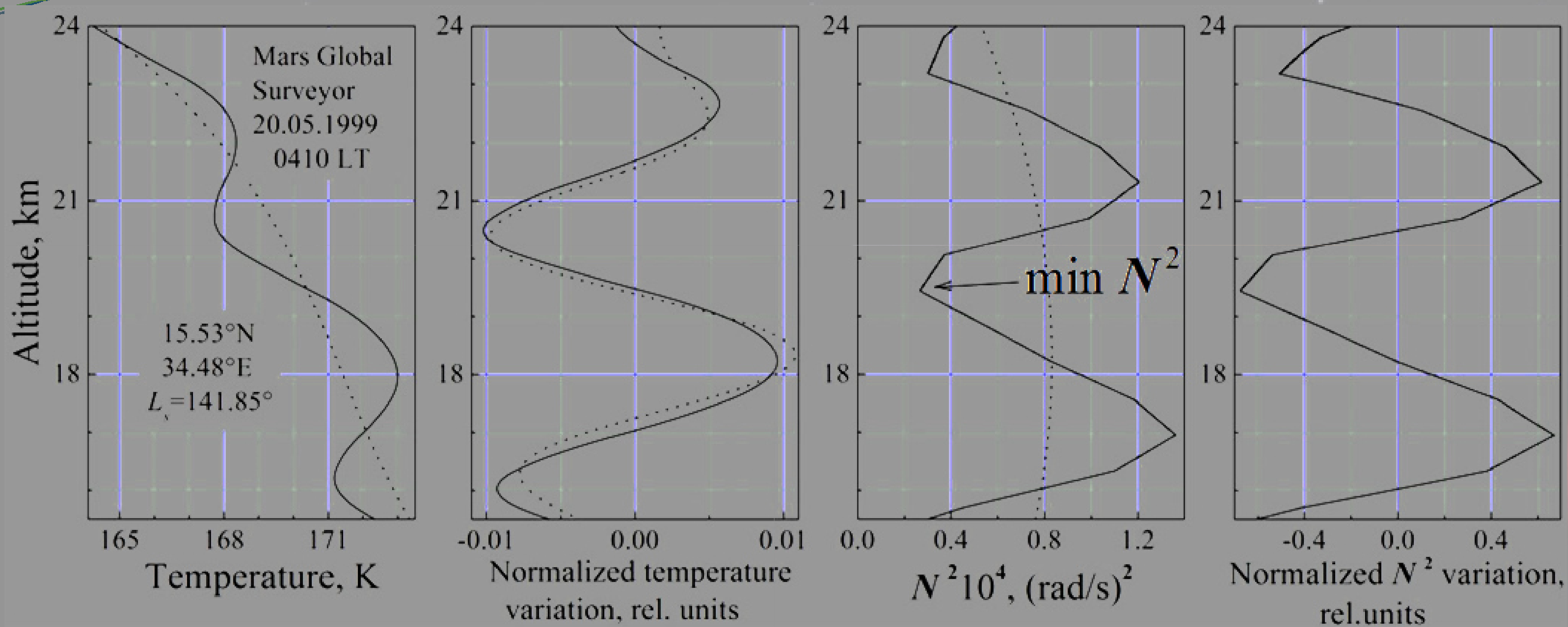

Figure 6. The same as Figure 5 except from radio occultation (data file: 9140V32A.TPS) conducted in summer (L_s=141.85°) at 04:10 h LT on 20 May 1999. Example of “clean” wave observations, where noise was not discovered in the spectrum of analyzed temperature fluctuations. **Wave parameters:** λ_z=4.5 km; λ_h=2080 km; E=39.9 J/kg; $p=E_k/E_p$=8.4; E_p=4.2 J/kg; f/ω=0.89; $T^{in}=2\pi/\omega$=40.7 hrs; a_e=0.63; $|u'|$=8.9 m/s; $|v'|$=7.9 m/s **[*Gubenko et al.*, 2015].**

Table 1. Internal wave parameters found from an analysis of *CHAMP* and *MARS GLOBAL SURVEYOR* RO temperature profiles in the six regions of planetary atmospheres. The coordinates of sounded regions, time and altitude intervals of observations are indicated. Uncertainties of determined parameters (Earth & Mars) are shown when they are less than 100%

Satellite	CHAMP ingress EARTH ingress		Mars Global Surveyor ingress MARS ingress		Mars Global Surveyor ingress MARS ingress	
IGW parameters	07 April 2001 06 h 51 m UT 84.2° S 83.2° E [25.5÷32.0] km	15 January 2002 21h 39 m UT 66.8° N 112.4° W [9.2÷16.7] km	28 January 1998 05 h 35 m LT 25.28° N, 127.19° E [15.0÷33.0] km	13 May 1999 04 h 13 m LT 26.74° N, 95.14° W [13.0÷31.0] km	19 May 1999 04 h 10 m LT 18.1° N 112.7° W [8.0÷26.5] km	20 May 1999 04 h 10 m LT 15.5° N 34.5° E [15.5÷24.0] km
λ_z, km	2.2 ± 0.7	2.1 ± 0.6	6.8 ± 0.6	8.2 ± 0.7	6.6 ± 0.6	4.5 ± 0.7
$\lvert\hat{T}\rvert$, 10^{-3} rel. units	6.5 ± 1.3	5.4 ± 1.2	10.8 ± 1.2	15.0 ± 1.7	19.0 ± 1.4	10.0 ± 1.7
$N_b^2, 10^{-4}\,\mathrm{rad}^2\mathrm{s}^{-2}$	4.5 ± 0.8	4.5 ± 0.7	0.60 ± 0.34	0.75 ± 0.41	0.7 ± 0.5	0.8 ± 0.4
$N_{min}^2, 10^{-4}\,\mathrm{rad}^2\mathrm{s}^{-2}$	2.5	2.7	0.12	0.18	0	0.3
a_e, rel. units	0.41 ± 0.17	0.36 ± 0.27	0.61 ± 0.36	0.57 ± 0.32	0.95 ± 0.64	0.63 ± 0.34
$A_{N^2}^{rel}$, rel.units	0.45	0.40	0.80	0.76	1	0.63
f/ω, rel. units	0.97 ± 0.04	0.98 ± 0.13	0.90 ± 0.18	0.92 ± 0.14	0.4	0.89 ± 0.19
ω, 10^{-4} rad s^{-1}	1.5 ±0.1	1.4 ± 0.2	0.68 ± 0.14	0.70 ± 0.11	1.1	0.4 ± 0.1
T^{in}, hours	11. 6 ± 0.4	13 ± 2	25.8 ± 5.3	25.0 ± 3.8	17	41 ± 9
$\lvert u'\rvert$, m s^{-1}	11.8 ± 4.1	11.4 ± 2.9	11.7 ± 4.6	16.1 ± 5.9	9.2 ± 6.5	8.9 ± 3.4
$\lvert v'\rvert$, m s^{-1}	11.5 ± 4.1	11.1 ± 3.2	10.5 ± 5.8	14.7 ± 7.0	3.9	7.9 ± 4.3
$\lvert w'\rvert$, 10^{-3} m s^{-1}	21 ± 12	16	45.1 ± 35.7	52.2 ± 37.8	105	20 ± 15
$\lvert C_{ph}^{in}\rvert$, m s^{-1}	29 ± 18	32 ± 9	19.1 ± 17.0	28.1 ± 23.7	9.7	14 ± 12
$\lvert C_{pz}^{in}\rvert$, 10^{-3} m s^{-1}	53 ± 17	45 ± 16	73.6 ± 16.4	91.2 ± 15.8	110	31 ± 8
λ_h, km	1230 ± 790	1450 ± 460	1770	2520 ± 2490	580	2080
E_p, m^2 s^{-2}	2.3 ± 1.0	1.5 ± 1.3	6.7 ± 4.1	10.4 ± 6.2	18 ± 12	4.2 ± 2.5
E, m^2 s^{-2}	70 ± 48	65 ± 22	68.6 ± 53.8	129 ± 95	43	40 ± 30
$p = E_k/E_p$, rel. units	30 ± 25	41 ± 10	9.2	11.4	1.4	8.4

ЗАКЛЮЧЕНИЕ

- Разработан оригинальный метод идентификации дискретных волновых событий и определения характеристик внутренних гравитационных волн на основе анализа вертикального профиля температуры, плотности или квадрата частоты Брента-Вяйсяля в атмосфере планеты **[*Gubenko et al.*, 2008a, 2011, 2012]**. Сформулирован и обоснован пороговый критерий идентификации ВГВ, в случае выполнения которого анализируемые флуктуации могут рассматриваться как волновые проявления в атмосфере.
- Применение разработанного метода к анализу вертикальных профилей температуры, восстановленных из радиозатменных измерений миссии *MARS GLOBAL SURVEYOR*, дало возможность идентифицировать ВГВ в атмосфере Марса и определить величины ключевых волновых характеристик, таких как собственная частота, амплитуды вертикальных и горизонтальных возмущений скорости ветра, вертикальная и горизонтальная длина волны, плотность кинетической и потенциальной энергии, вертикальные потоки волновой энергии и горизонтального импульса **[*Gubenko et al.*, 2015]**. В атмосфере планеты над районом Фарсиды впервые идентифицирована внутренняя гравитационная волна, степень насыщения которой составляет не менее 95%. Обнаруженные в атмосфере Марса ВГВ с вертикальной длиной волны 4.5–8.2 км являются волнами с низкими собственными частотами, близкими к инерционной частоте, а их кинетическая энергия, как правило, на порядок превышает потенциальную энергию. Распространение этих волн вызывает значительную модуляцию вертикальной стабильности атмосферной стратификации, что приводит к сдвиговой неустойчивости и возникновению тонких регулярных слоев перемежающейся турбулентности в атмосфере Марса.
- Работа выполнена при частичной финансовой поддержке Программы №7 Президиума РАН «Экспериментальные и теоретические исследования объектов Солнечной системы и планетных систем звезд. Переходные и взрывные процессы в астрофизике».

ЛИТЕРАТУРА

Creasey J.E., Forbes J.M., Hinson D.P. (2006). Global and seasonal distribution of gravity wave activity in Mars' lower atmosphere derived from MGS radio occultation data // Geophys. Res. Lett., Vol. 33, No. L01803, DOI: 10.1029/2005GL024037.

Fritts D.C. (1989). A review of gravity wave saturation processes, effects, and variability in the middle atmosphere // Pure Appl. Geophys., Vol. 130, P. 343–371.

Fritts D.C., Wang L., Tolson R.H. (2006). Mean and gravity wave structures and variability in the Mars upper atmosphere inferred from Mars Global Surveyor and Mars Odyssey aerobraking densities // J. Geophys. Res. 2006. Vol. 111. No. A12304, DOI: 10.1029/2006JA011897.

Gubenko V.N., Pavelyev A.G., Andreev V.E. (2008a). Determination of the intrinsic frequency and other wave parameters from a single vertical temperature or density profile measurement // J. Geophys. Res., Vol. 113, No. D08109, DOI: 10.1029/2007JD008920.

Gubenko V.N., Andreev V.E., Pavelyev A.G. (2008b). Detection of layering in the upper cloud layer of Venus northern polar atmosphere observed from radio occultation data // J. Geophys. Res. 2008. Vol. 113. No. E03001, DOI: 10.1029/2007JE002940.

Gubenko V.N., Pavelyev A.G., Salimzyanov R.R., Pavelyev A.A. (2011). Reconstruction of internal gravity wave parameters from radio occultation retrievals of vertical temperature profiles in the Earth's atmosphere // Atmos. Meas. Tech., Vol. 4, No. 10, P. 2153–2162, DOI: 10.5194/amt-4-2153-2011.

Gubenko V.N., Pavelyev A.G., Salimzyanov R.R., Andreev V.E. (2012). A method for determination of internal gravity wave parameters from a vertical temperature or density profile measurement in the Earth's atmosphere // Cosmic Research, Vol. 50, No. 1, P. 21–31, DOI: 10.1134/S0010952512010029.

Gubenko V.N., Kirillovich I.A., Pavelyev A.G. (2015). Characteristics of internal waves in the Martian atmosphere obtained on the basis of an analysis of vertical temperature profiles of the Mars Global Surveyor mission // Cosmic Research, Vol. 53, No. 2, P. 133–142, DOI: 10.1134/S0010952515020021.

Hinson D.P., Tyler G.L., Hollingsworth J.L., Wilson R.J. (2001). Radio occultation measurements of forced atmospheric waves on Mars // J. Geophys. Res., Vol. 106, No. E1, P. 1463–1480.

Спасибо за внимание!